

# Study on the Inhibition of PLD on IAV-induced Pulmonary Macrophage Based on Autophagy and Apoptosis

Ling Li, Yi Ning<sup>1</sup>, Ke Wei<sup>1</sup>, Jue Hu<sup>2</sup>, Tao Wu<sup>2</sup>, Cheng Zhao<sup>2</sup>, Fang-Guo Lu<sup>1</sup>, Qing-Hu He<sup>3</sup>

Department of Experimental Center for Medical Basic Teaching, The College of Traditional Chinese Medicine, <sup>1</sup>Department of Microbiology, The Medicine School, <sup>2</sup>Department of Postgraduate, Graduate School, <sup>3</sup>Laboratory of Integrated Chinese and Western Medicine, The College of Integrated Chinese and Western Medicine, Hunan University of Chinese Medicine, Changsha, Hunan, China

Submitted: 10-05-2019

Revised: 01-07-2019

Published: 11-02-2020

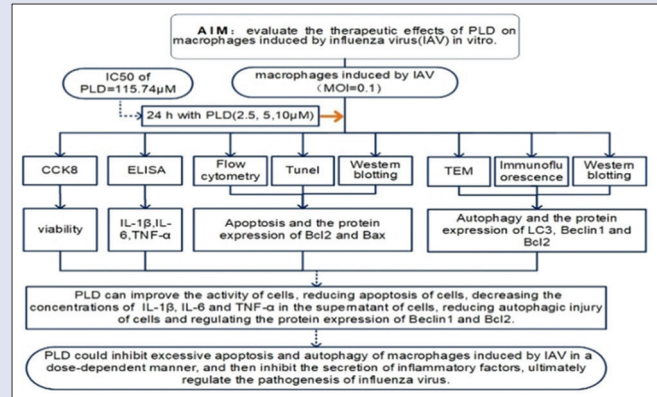
## ABSTRACT

**Background:** Platycodin D (PLD) comes from the main triterpenoid saponins in the dry roots of *Platycodon grandiflorum*, which has been used in traditional Chinese medicine in the treatment of respiratory disease. This study aimed to evaluate the therapeutic effects of PLD on mouse alveolar macrophages induced by influenza A virus (IAV) *in vitro* and to investigate the PLD of its action. **Materials and Methods:** Raw264.7 mouse alveolar macrophages were grown in culture and the Cell Counting Kit-8 assay determined cell viability. Cells were treated for 24 h with increasing doses of PLD (0, 5, 10, 20, 40, 60, 80, 100  $\mu$ M). The apoptosis was detected by Annexin V-FITC/PI and TUNEL assay. Levels of interleukin (IL)-1 $\beta$ , IL-6 and tumor necrosis factor (TNF)- $\alpha$  of supernatants were assessed using enzyme-linked immunosorbent assay. The numbers of phagophores, autophagosomes, and autolysosomes and the ultrastructure of cells were assessed using transmission electron microscope assay. The relative protein expression of microtubule-associated protein light chain (LC) 3I, LC3II, Beclin-1, and B cell lymphoma (Bcl2) was evaluated by Western blotting. The localizations of Beclin-1 and Bcl2 were viewed with a fluorescence microscope. **Results:** PLD treatment resulted in significant dose-dependent inhibition of the growth of Raw264.7 cells with the half-maximal inhibitory concentration of 115.74  $\mu$ M at 24 h. After Raw264.7 cells infected by influenza virus, PLD (2.5, 5, and 10  $\mu$ M) can improve the activity of cells, reducing apoptosis of cells, decreasing the concentrations of IL-1 $\beta$ , IL-6, and TNF- $\alpha$  in the supernatant of cells, reducing autophagic injury of cells and regulating the protein expression of Beclin-1 and Bcl2. **Conclusion:** PLD could inhibit excessive apoptosis and autophagy of macrophage cells induced by IAV in a dose-dependent manner and then inhibits the secretion of inflammatory factors caused by influenza virus infection caused by apoptosis and autophagy and then ultimately regulate the pathogenesis of influenza virus.

**Key words:** Apoptosis, autophagy, influenza virus, macrophages, platycodin D

## SUMMARY

To sum-up, platycodin D could inhibit excessive apoptosis and autophagy of macrophage cells induced by influenza virus in a dose-dependent manner. Thus, ultimately regulate the pathogenesis of influenza virus, which was probably through up-regulating the expression of Bcl2, down-regulating the expression of Beclin1, Bcl2-associated X protein and inhibits the secretion of inflammatory factors caused by influenza virus infection caused by apoptosis and autophagy and then ultimately regulate the pathogenesis of influenza virus. However, detailed mechanism of action remains to be studied.



**Abbreviations used:** PLD: Platycodin D; IAV: Influenza A virus; MOI: Multiplicity of infection; IL-1 $\beta$ : Interleukin-1 $\beta$ ; IL-6: Interleukin-6; TNF- $\alpha$ : Tumor necrosis factor- $\alpha$ ; ELISA: Enzyme-linked immunosorbent assay; TEM: Transmission electron microscope; IC<sub>50</sub>: The half-maximal inhibitory concentration; PBS: Pico base station; 4% PFA: Polar formation algorithm; BCA: Bladder cancer; ECL: Electrochemiluminescence; LC3: Microtubule-associated protein light chain 3; Beclin-1: Beclin1; Bcl2: B-cell lymphoma/leukemia-2; Bax: Bcl2-associated X protein.

## Correspondence:

Prof. Fang-Guo Lu,  
Department of Microbiology, The Medicine School, Hunan University of Chinese Medicine, Xueshi Road 300, Changsha, Hunan 410208, China.

E-mail: lufanguo0731@163.com

Prof. Qing-Hu He,  
Laboratory of Integrated Chinese and Western Medicine, The College of Integrated Chinese and Western Medicine, Hunan University of Chinese Medicine, Changsha, Hunan, China.

E-mail: qinghu\_he@foxmail.com

DOI: 10.4103/pm.pm\_207\_19

Access this article online

Website: www.phcog.com

Quick Response Code:



## INTRODUCTION

Influenza virus (IAV) is a highly transmitted common respiratory pathogen, and it can lead to seasonal and periodic global influenza epidemics.<sup>[1]</sup> According to the latest data of the WHO in February 2019, there are high levels of influenza epidemics in many countries and regions around the world, with influenza A accounting for more than 60%. The more serious pathogenicity of influenza A virus and the more complex mechanism of action is a major reason.<sup>[2,3]</sup> Autophagy is one of the pathways through which the body degrades intracellular

This is an open access journal, and articles are distributed under the terms of the Creative Commons Attribution-NonCommercial-ShareAlike 4.0 License, which allows others to remix, tweak, and build upon the work non-commercially, as long as appropriate credit is given and the new creations are licensed under the identical terms.

For reprints contact: reprints@medknow.com

Cite this article as: Li L, Ning Y, Wei K, Hu J, Wu T, Zhao C, *et al.* Study on the inhibition of PLD on IAV-induced pulmonary macrophage based on autophagy and apoptosis. *Phcog Mag* 2020;16:132-9.

damaged proteins and macromolecules under normal conditions. However, autophagy is a double-edged sword. Autophagy plays a vital role during influenza A virus infection.<sup>[4-7]</sup> When influenza viruses invade, they induce autophagy of host cells, which further aggravates the pathogenicity of influenza viruses, and autophagy plays a vital role in regulating the production of cytokines during influenza A virus infection. In the apoptotic family, B lymphoma-2 (Bcl2) can bind with autophagy-related protein 6 (Atg6, also known as Beclin-1) to form a Beclin1-Bcl2 polymer, which can inhibit autophagy.<sup>[8,9]</sup>

Although Western medicine plays a leading role in anti-influenza, the large demand for mainstream drugs increases the risk of mutation and drug resistance of influenza viruses. Because of antigenic variation, the preventive effect of common vaccines is also affected.<sup>[10-12]</sup> Therefore, it has been a top priority for the antiviral industry to continue to study the pathogenesis and mutation mechanism of influenza viruses and to find or develop new and more effective anti-influenza drugs.

China has a heritage of many classic traditional Chinese medicine compounds derived from the fighting of diseases for thousands of years, making diseases well treated and controlled.<sup>[13]</sup> Especially in influenza prevention and control, it has obvious advantages. Platycodin D (PLD) comes from the main triterpenoid saponins in the dry roots of *Platycodon grandiflorum*, which has been used in traditional Chinese medicine in the treatment of respiratory disease. The main pharmacological activities of PLD are anti-inflammatory, expectorant, antitussive, sedative, analgesic, and antipyretic.<sup>[14-16]</sup> The effect of PLD in inhibition of the cell damage induced by IAV and the specific roles of PLD in autophagy remain unclear. To clarify that issue, we investigated the effects of PLD on autophagy and progression in macrophages induced by IAV in this study.

## MATERIALS AND METHODS

### Cell culture and the influenza virus

Raw264.7 macrophages were derived from the American Type Culture Collection, it was cultured and preserved in our laboratory. The cells were maintained in RPMI 1640 medium (Hyclone, China) containing with 10% fetal bovine serum (Hyclone, China) under 5% CO<sub>2</sub> at 37°C. The influenza virus (type A, IAV, A/PR/8/34) was provided by the Virus Research Laboratory of Hunan Normal University. After 10 days of culture and passage in the allantoic cavity of 10-day-old chick embryo, the viruses with a titer of more than 1:640 were used for the study.

### The half-maximal inhibitory concentration of platycodin D

Raw264.7 cells were seeded into 96-well plates (6000 cells/well). Then, the cells were incubated with different concentrations (0,5,10,20,40,60,80,100 μM) of PLD D (PLD, Shanghai Yuanye Biotechnology Co., Ltd. Shanghai, China) were used for 24 h, respectively. The cytotoxicity was measured using the Cell Counting Kit-8 (CCK-8) assay (7sea, China) according to the kit instructions. The optical densities (ODs) were measured at absorbance 450 nm. The cell inhibition rate (IR) was calculated according to the OD as follows: IR (%) = 1 - (OD treatment group / OD control group) × 100%.

### Cell viability analysis by Cell Counting Kit-8

Raw264.7 cells were seeded into 96-well plates (6000 cells/well). Then, the cells were stimulated by IAV (multiplicity of infection [MOI] = 0.1) for 12 h and incubated with PLD (2.5, 5, 10 μM) for 24 h. After that, the cell activity was examined by CCK8 assay. The percentage of cell viability was calculated according to the OD as follows: cell viability (%) = (OD treatment group / OD control group) × 100%.

### Enzyme-linked immunosorbent assay

Raw264.7 cells were seeded into 6-well plates (8000 cells/well). Following different treatments approach the same as before, the cells were collected supernatant of different groups, secretion levels of interleukin-1beta (IL-1 β), IL 6 and tumor necrosis factor-alpha (TNF-α) (eBioscience, USA) were assessed using enzyme-linked immunosorbent assay (ELISA), according to the manufacturer's instructions.

### Cell apoptosis analysis by flow cytometry

Raw264.7 cells were seeded into 6-well plates (10,000 cells/well). Following different treatments approach the same as before, the cells were collected and detected using annexin V-FITC and propidium iodide kit. The apoptotic percentages of the treated cells were analyzed by flow cytometry using a Beckman Coulter CytExpert.

### TUNEL assay

Raw264.7 cells were seeded into 6-well plates (8000 cells/well). Following different treatments approach the same as before, the number of apoptotic cells was detected using TdT-mediated dUTP-biotin nick end labeling assay (TUNEL). The number of positive cells was calculated in five fields of view selected at random for each cell sample by biological microscope (CX31, Olympus). The integrated OD of samples was analyzed using Image-Pro Plus 6.0 software. (Media Cybernetics, Maryland, USA).

### Transmission electron microscope

Raw264.7 cells were seeded into 6-well plates (8000 cells/well). Following different treatments approach the same as before, the cells were collected and fixed with 2.5% glutaraldehyde for 2 h at 4°C and by 1% osmic acid. Then, the cells were carried out at room temperature (RT) in a graded series of 50%, 70%, and 90% acetone and soaked in propylene epoxide and resin for embedding and subsequent polymerization. 50–100 nm ultrathin sections of specimens were made with an ultramicrotome and a diamond knife. After 3% uranyl acetate and lead nitrate double staining, the specimens were examined and photographed on an electron microscope (HITACHIHT7700, Japan).

### Immunofluorescence

Raw264.7 cells were seeded into 6-well plates (8000 cells/well). Following different treatments approach the same as before, the cells were collected and fixed with 4% polar formation algorithm for 30 min at 4°C and washed three times by cold pico base station (PBS). The cells were incubated with primary antibodies (Beclin-1 and bcl2) at 4°C overnight then incubated with goat anti-mouse Alexa-594 (1:500; Invitrogen, Carlsbad, CA, USA) or goat anti-rabbit Alexa-488 (1:500; Invitrogen). Immunofluorescence was viewed with a fluorescence microscope (LSM780, Zeiss, Germany). Five visual fields of each sample were randomly selected and analyzed at a high magnification. The fluorescence intensity of each group was analyzed statistically.

### Western blotting

Raw264.7 cells were seeded into 6-well plates (8000 cells/well). Following different treatments approach the same as before, the cells were washed by cold PBS and completely lysed by lysis buffer (CW BIO, China) containing protease inhibitor mixture. The concentration of protein was determined using the BCA kit (CW BIO, China), and 50 μg of total protein sample was loaded for sodium dodecyl sulfonate-polyacrylamide gel electrophoresis (SDSPAGE) electrophoresis. Then, protein samples were separated by 10%

SDS-polyacrylamide gel and transferred onto polyvinylidene difluoride membrane with a diameter of 0.22 m. The membrane was blocked in the blocking buffer for 1 h and incubated with primary antibodies: microtubule-associated protein light chain (LC) 3 Rabbit antibody (Ab), Bcl2 mouse Ab, Beclin-1 Rabbit Ab and  $\beta$  Rabbi mouse Ab (1:1000) at 4°C overnight and anti-mouse or anti-rabbit secondary antibodies (1:3000) for 1 h at RT. After electrochemiluminescence, the blots were examined by A Bio-Rad Gel Dol EZ imager (Bio-Rad, USA), and the images and the relative protein expression was analyzed with Image Lab 5.0 software (Bio-Rad, USA) for statistical analysis.

### Statistical analysis

Measurement data are expressed as mean  $\pm$  standard deviation ( $\bar{x} \pm s$ ), data were tested for homogeneity of variance. When the variance was homogeneous, one-way ANOVA test was used, and multiple comparisons were made among groups. When the variance is uneven, Kruskal–Wallis H test is used to compare the total difference, and Mann–Whitney U test is used to compare the difference between the two groups. Data were processed using SPSS 21.0 statistical software (SPSS, USA), and significance was determined as  $P < 0.05$ .

## RESULTS

### The half-maximal inhibitory concentration of platycodin D

The PLD inhibited Raw264.7 cells proliferation *in vitro* was examined by CCK8 assay [Figure 1a]. As shown in chart, PLD inhibited Raw264.7 cells proliferation *in vitro* in concentration-dependent manners with the half-maximal inhibitory concentration values of 115.74  $\mu$ M at 24 h, respectively.

### Platycodin D improving the activity of cells infected by influenza virus

The cell activity was examined by CCK8 assay [Figure 1b]. IAV resulted in significantly decreased cell viability compared with the control group ( $P < 0.05$ ); however, the cell viability of Raw264.7 cells stimulated by IAV (MOI = 0.1) were significantly higher than those of PLD (2.5, 5, 10  $\mu$ M) ( $P < 0.05$ ) and the viability of PLD presented an approximate dose-dependent manner.

### Platycodin D decreasing the concentrations of interleukin-1 $\beta$ , interleukin-6 and tumor necrosis factor- $\alpha$ in the supernatant of cells infected by influenza virus

The concentrations of IL-1  $\beta$ , IL-6, and TNF- $\alpha$  in the supernatant were examined by ELISA assay [Figure 2]. IAV resulted in significantly increased the concentrations of IL-1  $\beta$ , IL-6, and TNF- $\alpha$  in the supernatant compared with the control group ( $P < 0.05$ ); however, this influence of IAV were significantly inhibited by those of PLD (2.5, 5, 10  $\mu$ M) ( $P < 0.05$ ) and the curative effect of PLD presented an approximate dose-dependent manner.

### Platycodin D reducing apoptosis of cells infected by influenza virus

The apoptotic percentages were examined by flow cytometry assay [Figure 3]. IAV resulted in significantly accelerated apoptotic percentages compared with the control group ( $P < 0.05$ ); however, this influence of IAV was significantly inhibited by those of PLD (2.5, 5, 10  $\mu$ M) ( $P < 0.05$ ) and the curative effect of PLD presented an approximate dose-dependent manner. The apoptosis of the PLD-treated cells was further confirmed by TUNEL assay [Figure 4].

### Platycodin D regulating the protein expression of Bcl2 and Bcl-2-associated X protein

The protein expression of Bcl2 and Bcl-2 associated X protein (Bax) was examined by Western blotting [Figure 5]. IAV resulted in significantly up-regulated the protein expression of Bax and down-regulated the protein expression of Bcl2, compared with the control group ( $P < 0.05$ ); however, this influence of IAV were significantly inhibited by those of PLD (2.5, 5, 10  $\mu$ M) ( $P < 0.05$ ) and the curative effect of PLD presented an approximate dose-dependent manner.

### Platycodin D reducing excessive autophagy of cells infected by influenza virus

Evaluate the ultrastructure within cells to analyze the effect of PLD during IAV-induced autophagic injury by TEM assay [Figure 6]. Numbers of phagophores, autophagosomes, and autolysosomes increased in the IAV

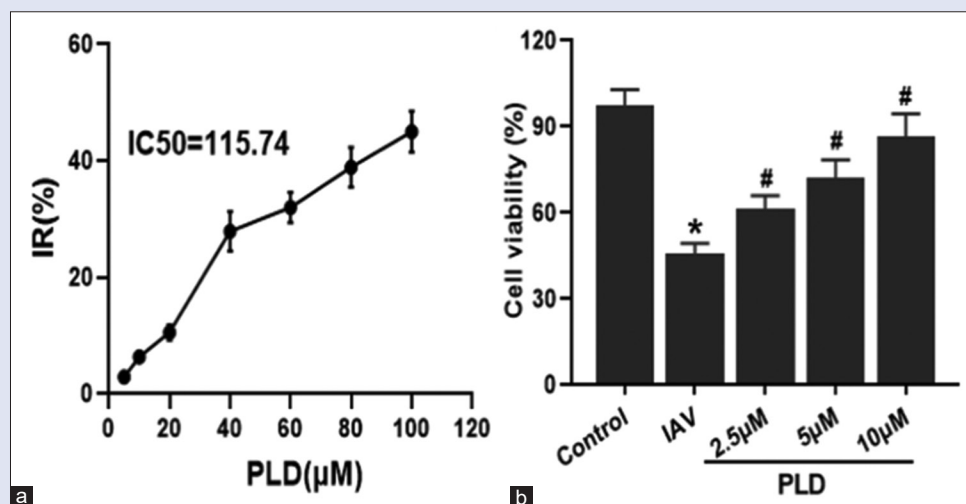


**Figure 1:** (a) The half-maximal inhibitory concentration of platycodin D were examined by Cell Counting Kit 8 assay,  $n = 5$ . (b) The cell activity were examined by Cell Counting Kit 8 assay,  $n = 5$ . \* $P < 0.05$  versus control group; # $P < 0.05$  versus IAV group; PLD: Platycodin D; IAV: Influenza A virus (multiplicity of infection = 0.1). Data are expressed as the mean  $\pm$  standard deviation

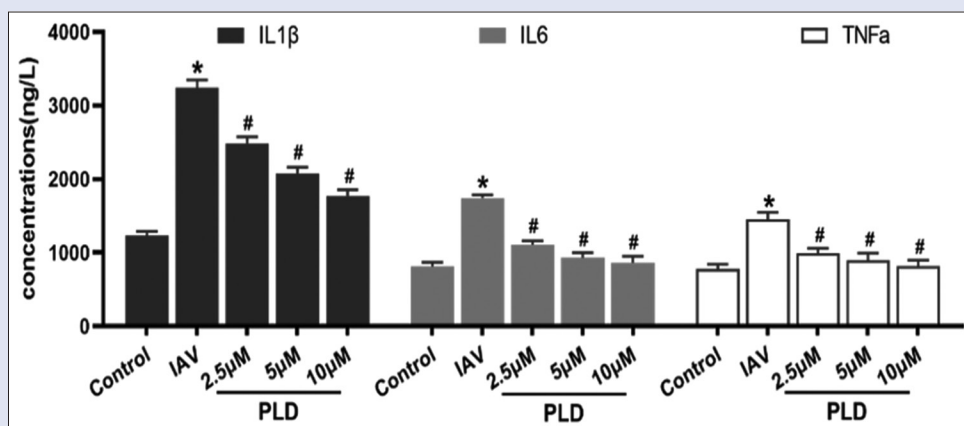


**Figure 2:** The concentrations of interleukin-1 $\beta$ , interleukin-6 and tumor necrosis factor- $\alpha$  in the supernatant by enzyme-linked immunosorbent assay.  $n = 5$ . \* $P < 0.05$  versus control group; # $P < 0.05$  versus IAV group; PLD: Platycodin D; IAV: Influenza A virus (multiplicity of infection = 0.1). Data are expressed as the mean  $\pm$  standard deviation

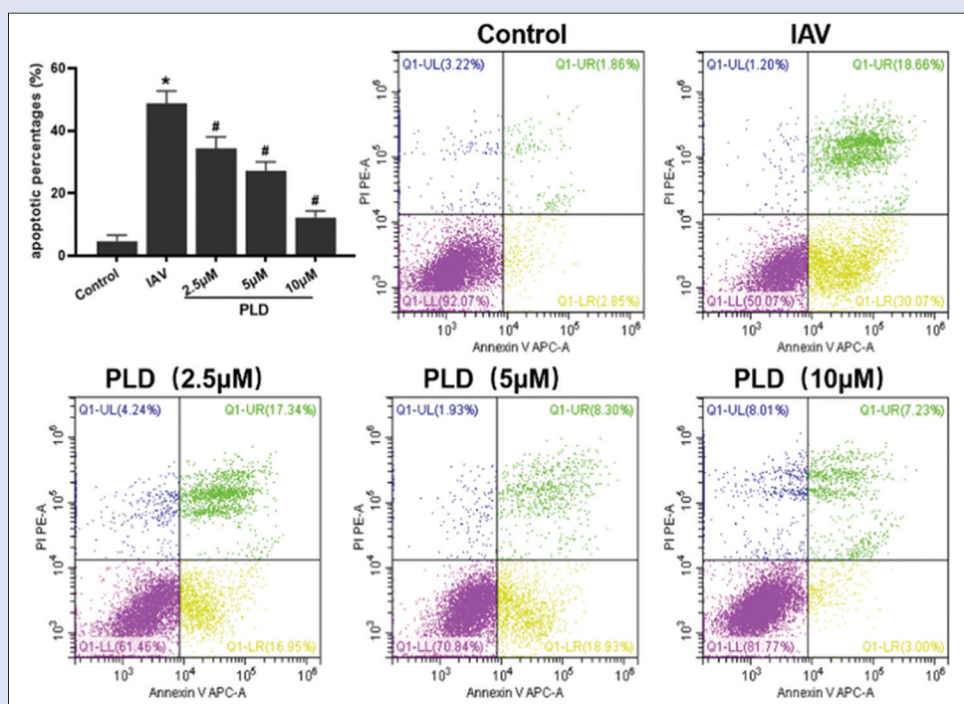


**Figure 3:** The apoptotic percentages were examined by flow cytometry assay,  $n = 5$ . \* $P < 0.05$  versus control group; # $P < 0.05$  versus IAV group; PLD: Platycodin D; IAV: Influenza A virus (multiplicity of infection = 0.1). Data are expressed as the mean  $\pm$  standard deviation

group, at the same time, the ultrastructure of mitochondria swelled, the structure was destroyed, vacuoles increased, nuclear pyknosis, and so on. However, PLD treatments are able to decrease the numbers of phagophores, autophagosomes, and autolysosomes and protect the ultrastructure of cells. These results indicated that PLD decreased IAV-induced excessive autophagy, and the curative effect of PLD presented an approximate dose-dependent manner. The proteins related with autophagy (LC3II/LC3I and Beclin-1) were further confirmed by Western blotting [Figure 7].

### Platycodin D regulating the balance of Beclin-1 and Bcl2

Endogenous Beclin-1 and Bcl2 were localized in the cytoplasm [Figure 8]. The localization was dramatically decreased when IAV was added to the

medium, and the relative protein expression of Beclin-1 was increased, then autophagy was promoted. However, it decreased following PLD treatment. These results indicated that PLD decreased IAV-induced autophagic injury by regulated the protein expression of Beclin-1 and Bcl2. Furthermore, the curative effect of PLD presented an approximate dose-dependent manner.

### DISCUSSION

In the process of influenza virus infection, pulmonary epithelial cells act as the first line of defense against influenza virus infection, quickly respond to influenza virus infection, and activate alveolar macrophages. Activated alveolar macrophages are produced by cytokines such as TNF- $\alpha$ , IL-1 $\beta$ , IL-6, and IL-8. Excessive immune

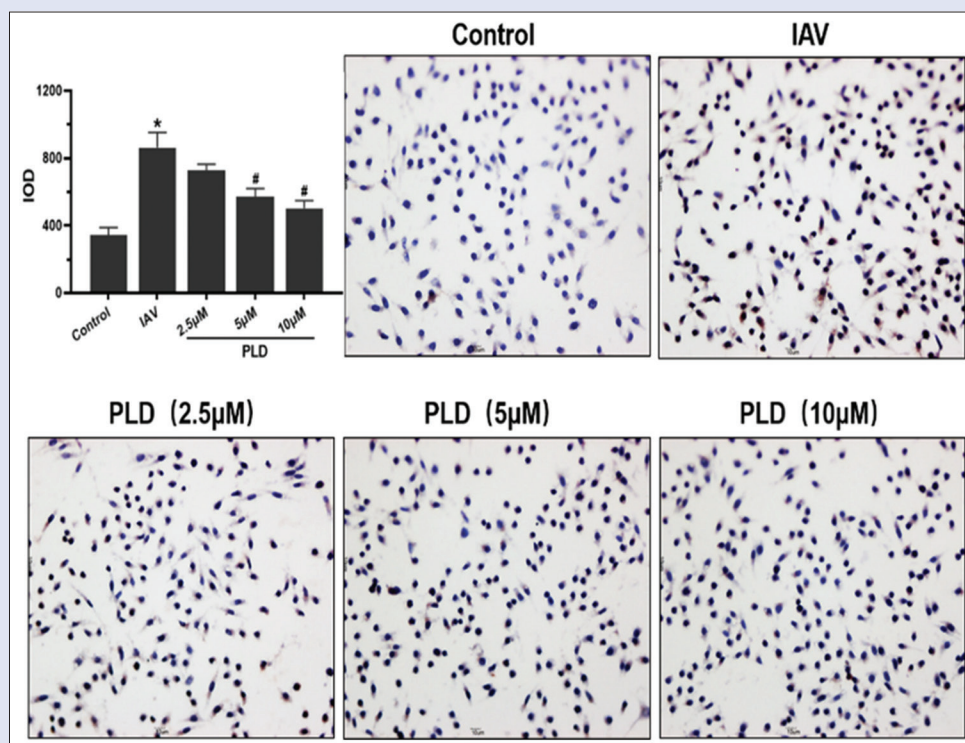


**Figure 4:** The integrated optical density by TUNEL assay,  $n = 5$ . \* $P < 0.05$  versus control group; # $P < 0.05$  versus IAV group; PLD: Platycodin D; IAV: Influenza A virus (multiplicity of infection = 0.1). Data are expressed as the mean  $\pm$  standard deviation

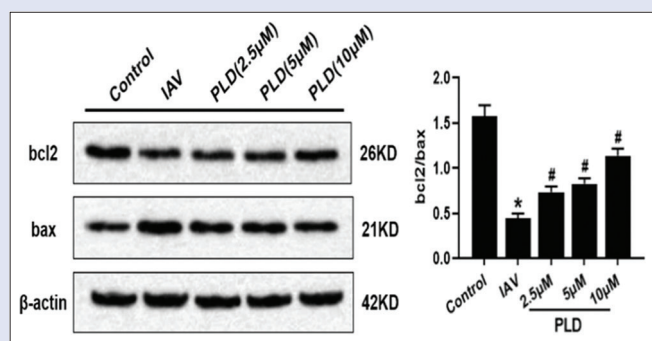


**Figure 5:** The proteins related with apoptosis (Bcl2 and Bcl-2 associated X protein) by Western blotting,  $n = 5$ . \* $P < 0.05$  versus control group; # $P < 0.05$  vs. IAV group; PLD: Platycodin D; IAV: Influenza A virus (multiplicity of infection = 0.1). Data are expressed as the mean  $\pm$  standard deviation

response leads to high level and sustained expression of cytokines. This “cytokine storm” ultimately causes alveolar macrophages to amplify inflammatory response, release, and spread and invade adjacent or distant host cells, accelerating the progression of lung injury. Some patients can rapidly evolve into severe progressive pneumonia, lung injury, and even acute respiratory distress syndrome.<sup>[17-19]</sup> In the present study, first, we demonstrated that PLD inhibited macrophage cells damage; second, supernatants of IAV-stimulated Raw264.7 cells in the presence of PLD were examined for the production of the proinflammatory cytokines, IL-1  $\beta$ , IL-6, and TNF- $\alpha$ . These proinflammatory cytokines significantly inhibited by PLD in a dose-dependent manner. These results were confirmed by treating Raw 246.7 cells with PLD at various doses after IAV-stimulated. These data indicate PLD may be interfering

with the signal transduction pathway of proinflammatory cytokines activation.

Apoptosis is widely considered to be the main mechanism regulating cell death, which is often initiated when cells are damaged or stressed. In the present study, we demonstrated that PLD inhibited excessive apoptosis of macrophage cells induced by IAV in a dose-dependent manner. PLD significantly increased expression of apoptosis inhibitor protein Bcl2 and decreased expression of apoptotic Bax, then regulated the balance between Bcl2/Bax.

Autophagy is an important mechanism underlying the interaction between influenza viruses and their hosts. Therefore, researchers have begun to pay attention to the complex relationship between influenza viruses infection and autophagy in recent years. More and more evidence shows that the influenza virus can cause autophagy, which is a necessary process of influenza virus replication.<sup>[5-7]</sup> In the present study, we demonstrated that PLD inhibited excessive autophagy of macrophage cells induced by IAV in a dose-dependent manner. PLD treatments are able to decrease the numbers of phagophores, autophagosomes and autolysosomes, protect the ultrastructure of cells and down-regulate the LC3II/LC3I ratio and the relative protein expression of Beclin-1. These results indicated that PLD decreased IAV-induced autophagic injury, and the curative effect of PLD presented an approximate dose-dependent manner.

Autophagy-related genes are the core molecular mechanism of autophagy. As one of the key molecules in autophagy formation, autophagy-related protein Beclin1 is the key target of autophagy regulation.<sup>[8,9]</sup> As an important autophagy inhibitor protein, Bcl2 protein in apoptotic family binds to Beclin-1 and inhibits its autophagy-promoting activity.<sup>[20,21]</sup> Under normal conditions, Beclin-1 binds to Bcl2 family proteins, including Bcl2, Bcl-XL, Bcl-w, and myeloid cell leukemia-1 and inhibits autophagy. Therefore, the formation and dissociation of Beclin-1-Bcl2 are crucial to the regulation of autophagy,<sup>[22]</sup> which is also regulated

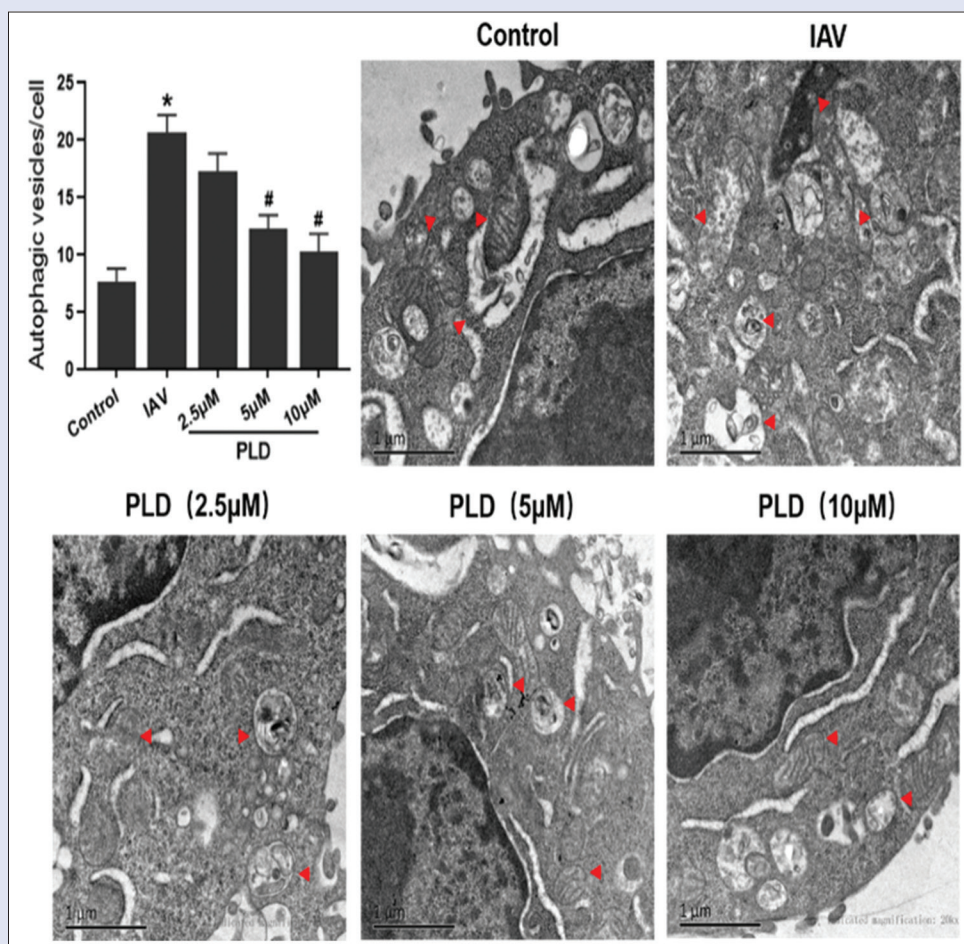


**Figure 6:** The result of electron-microscopy investigation by transmission electron microscope,  $n = 5$ . \* $P < 0.05$  versus control group; # $P < 0.05$  versus IAV group; PLD: Platydocin D; IAV: Influenza A virus (multiplicity of infection = 0.1). Data are expressed as the mean  $\pm$  standard deviation

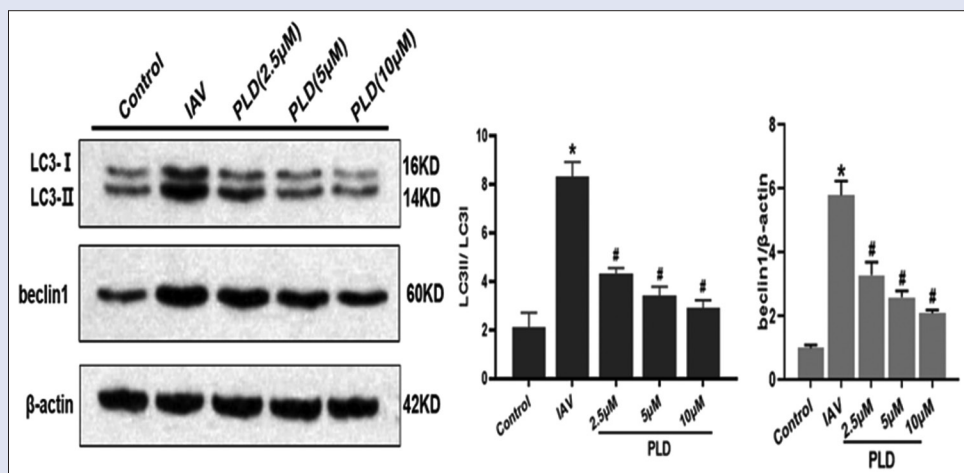


**Figure 7:** The proteins related with autophagy (microtubule-associated protein light chain 3II/microtubule-associated protein light chain 3I and Beclin1) by Western blotting,  $n = 5$ . \* $P < 0.05$  versus control group; # $P < 0.05$  versus IAV group; PLD: platydocin D; IAV: Influenza A virus (multiplicity of infection = 0.1). Data are expressed as the mean  $\pm$  standard deviation

by many proteins and signaling pathways. In the present study, we demonstrated that the localization and the relative protein expression of Beclin-1 and Bcl2. These data indicate PLD may be down-regulate

the relative protein expression of Beclin-1 and up-regulate the relative protein expression of Bcl2 after IAV-stimulated and the curative effect of PLD presented an approximate dose-dependent manner.

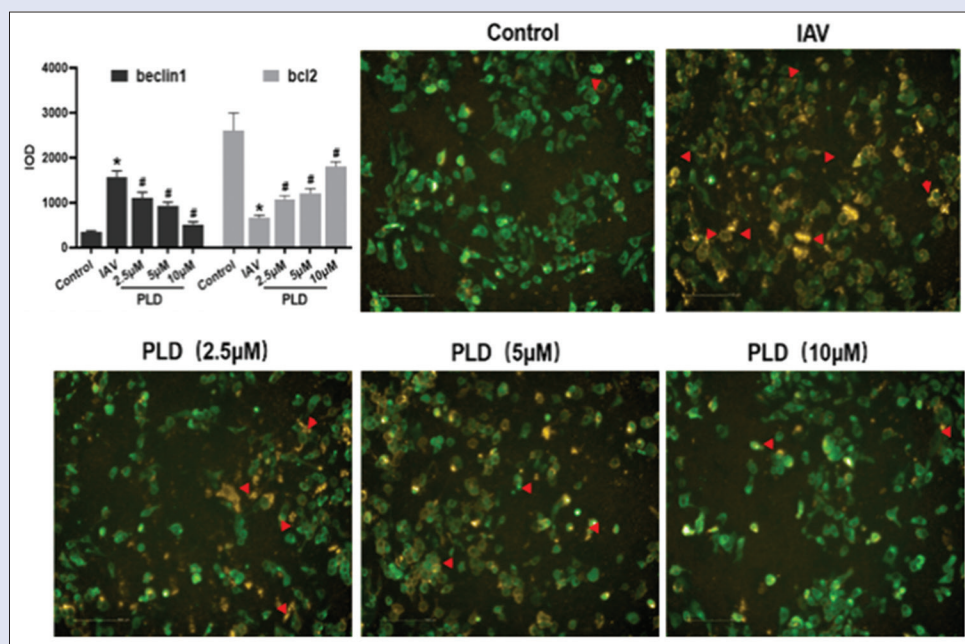


**Figure 8:** Cofocal imaging for autophagosome (subcellular localization of Beclin-1 and Bcl2) by Immunofluorescence,  $n = 5$ . \* $P < 0.05$  versus control group; # $P < 0.05$  versus IAV group; PLD: Platydocodin D; IAV: Influenza A virus (multiplicity of infection = 0.1). Data are expressed as the mean  $\pm$  standard deviation

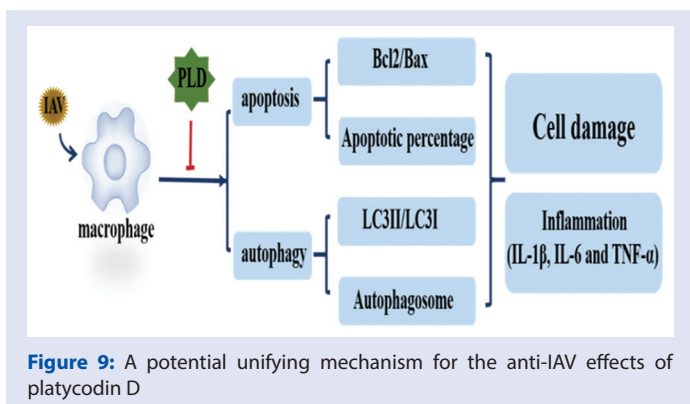


**Figure 9:** A potential unifying mechanism for the anti-IAV effects of platycodin D

## CONCLUSION

PLD could inhibit excessive apoptosis and autophagy of macrophage cells induced by IAV in a dose-dependent manner. Thus, ultimately regulate the pathogenesis of influenza virus, which was probably through upregulating the expression of Bcl2, down-regulating the expression of Beclin-1, Bax and inhibits the secretion of inflammatory factors caused by influenza virus infection caused by apoptosis and autophagy and then ultimately regulate the pathogenesis of influenza virus [Figure 9].

## Acknowledgements

The authors would like to thank Professor Chen Ze of Hunan Normal University for his support and help. In addition, the authors would like to thank the scientific and technological innovation team of colleges and universities in Hunan Province (Research on prevention and treatment of infectious diseases with traditional Chinese Medicine, No. 15).

## Financial support and sponsorship

This work is supported by grants from the National Nature Science Foundation of China (No. 81973670, 81503445, 81774126, 81703919

and 81803964), the Hunan Natural Science Foundation (No. 2016JJ2095). The Education Department of Hunan Province, the innovation platform of open fund project (No. 17K067).

## Conflicts of interest

There are no conflicts of interest.

## REFERENCES

1. Beumer MC, Koch RM, van Beuningen D, OudeLashof AM, van de Veerdonk FL, Kolwijck E, *et al.* Influenza virus and factors that are associated with ICU admission, pulmonary co-infections and ICU mortality. *J Crit Care* 2019;50:59-65.
2. Guo XJ, Thomas PG. New fronts emerge in the influenza cytokine storm. *Semin Immunopathol* 2017;39:541-50.
3. Liu Q, Zhou YH, Yang ZQ. The cytokine storm of severe influenza and development of immunomodulatory therapy. *Cell Mol Immunol* 2016;13:3-10.
4. Zhang R, Chi X, Wang S, Qi B, Yu X, Chen JL. The regulation of autophagy by influenza A virus. *Biomed Res Int* 2014;2014:498083.
5. Dreux M, Chisari FV. Viruses and the autophagy machinery. *Cell Cycle* 2010;9:1295-307.
6. Sir D, Ou JH. Autophagy in viral replication and pathogenesis. *Mol Cells* 2010;29:1-7.
7. Zhou Z, Jiang X, Liu D, Fan Z, Hu X, Yan J, *et al.* Autophagy is involved in influenza A virus replication. *Autophagy* 2009;5:321-8.
8. Beale R, Wise H, Stuart A, Ravenhill BJ, Digard P, Randow F. A LC3-interacting motif in the influenza A virus M2 protein is required to subvert autophagy and maintain virion stability. *Cell Host Microbe* 2014;15:239-47.
9. Münz C. Beclin-1 targeting for viral immune escape. *Viruses* 2011;3:1166-78.
10. Lee N, Hurt AC. Neuraminidase inhibitor resistance in influenza: A clinical perspective. *Curr Opin Infect Dis* 2018;31:520-6.
11. Shin WJ, Seong BL. Novel antiviral drug discovery strategies to tackle drug-resistant mutants of influenza virus strains. *Expert Opin Drug Discov* 2019;14:153-68.
12. Bhuiyan MU, Snelling TL, West R, Lang J, Rahman T, Granland C, *et al.* The contribution of viruses and bacteria to community-acquired pneumonia in vaccinated children: A case-control study. *Thorax* 2019;74:261-9.
13. Ling L, Bing D, Fangguo L, Xiaoge G, Bo Z, Qiang G, *et al.* Experimental study on the effect of different proportion of maxingshigan decoction on influenza virus infection in mice. *China J Tradit Chin Med Pharm* 2017;32:309-13.

14. Zhang M, Du T, Long F, Yang X, Sun Y, Duan M, *et al.* Platycodin D suppresses type 2 porcine reproductive and respiratory syndrome virus in primary and established cell lines. *Viruses* 2018;10. pii: E657.
15. Meng YL, Wang WM, Lv DD, An QX, Lu WH, Wang X, *et al.* The effect of platycodin D on the expression of cytoadherence proteins P1 and P30 in mycoplasma pneumoniae models. *Environ Toxicol Pharmacol* 2017;49:188-93.
16. Wang Z, Cai J, Fu Q, Cheng L, Wu L, Zhang W, *et al.* Anti-inflammatory activities of compounds isolated from the rhizome of *Anemarrhena asphodeloides*. *Molecules* 2018;23. pii: E2631.
17. Whitsett JA, Alenghat T. Respiratory epithelial cells orchestrate pulmonary innate immunity. *Nat Immunol* 2015;16:27-35.
18. Divangahi M, King IL, Pernet E. Alveolar macrophages and type I IFN in airway homeostasis and immunity. *Trends Immunol* 2015;36:307-14.
19. Kopf M, Schneider C, Nobs SP. The development and function of lung-resident macrophages and dendritic cells. *Nat Immunol* 2015;16:36-44.
20. Pattingre S, Tassa A, Qu X, Garuti R, Liang XH, Mizushima N, *et al.* Bcl-2 antiapoptotic proteins inhibit beclin 1-dependent autophagy. *Cell* 2005;122:927-39.
21. Erlich S, Mizrachy L, Segev O, Lindenboim L, Zmira O, Adi-Harel S, *et al.* Differential interactions between beclin 1 and bcl-2 family members. *Autophagy* 2007;3:561-8.
22. Dai JP, Zhao XF, Zeng J, Wan QY, Yang JC, Li WZ, *et al.* Drug screening for autophagy inhibitors based on the dissociation of beclin1-bcl2 complex using biFC technique and mechanism of eugenol on anti-influenza A virus activity. *PLoS One* 2013;8:e61026.